We are IntechOpen, the world's leading publisher of Open Access books Built by scientists, for scientists

4,800
Open access books available

122,000
International authors and editors

135M
Downloads

Our authors are among the

154
Countries delivered to

TOP 1%
most cited scientists

12.2%
Contributors from top 500 universities

CLARIVATE ANALYTICS BOOK CITATION INDEX INDEXED

WEB OF SCIENCE™

Selection of our books indexed in the Book Citation Index in Web of Science™ Core Collection (BKCI)

Interested in publishing with us?
Contact book.department@intechopen.com

Numbers displayed above are based on latest data collected.
For more information visit www.intechopen.com

Chapter 12

Effects of Inorganic Seeds on Secondary Organic Aerosol (SOA) Formation

Biwu Chu, Jingkun Jiang, Zifeng Lu, Kun Wang, Junhua Li and Jiming Hao

Additional information is available at the end of the chapter

http://dx.doi.org/10.5772/48424

1. Introduction

Atmospheric aerosol has significant influences on human health (Kaiser, 2005), visibility degradation (Cheng et al., 2011), and climate change (Satheesh and Moorthy, 2005). It was found that organic aerosols (OA) was the most abundant component of atmospheric aerosol (He et al., 2001) and more than 50% of the total OA are secondary organic aerosols (SOA) (Duan et al., 2005). SOA are produced from the oxidation of volatile organic compounds (VOCs) followed by gas-particle partitioning of the semivolatile organic products. Among the various VOCs, aromatic hydrocarbons are one type of SOA precursors which have drawn the most attention due to their abundance in the air and high SOA contribution to urban atmospheres (Lewandowski et al., 2008). Toluene and *m*-xylene are the two of the most abundant aromatic hydrocarbon species.

The detailed mechanism and controlling factors of SOA formation are not fully understood yet, which leads to the lower SOA level prediction from air quality models than the ambient measurements (Volkamer et al., 2006). Using smog chamber, SOA formation process can be investigated under controlled experimental conditions. Series of smog experiments have been conducted by different research groups to investigate the effects of background seed aerosols on SOA formation (Cao and Jang, 2007, Czoschke et al., 2003, Gao et al., 2004, Jang et al., 2002, Liggio and Li, 2008). Increased SOA formation and SOA yields were observed with the presence of acid seed aerosols. The effects of acidic seeds suggest that aerosol phase reactions may play an important role on SOA formation (Jang et al., 2002). Interactions between the organic and inorganic components of aerosols are important for further understanding the SOA formation process. Most research concludes that acid-catalyzed aerosol-phase reactions generate additional aerosol mass due to the production of oligomeric products with large molecular weight and extremely low volatility (Cao and Jang, 2007, Czoschke et al., 2003, Gao et al., 2004) and, therefore, enhance SOA formation.

Uptake of semivolatile organic products to acidic sulfate aerosols was also found contributing to enhance SOA formation (Liggio and Li, 2008). In these studies, $(NH_4)_2SO_4$ or H_2SO_4 seed aerosols were widely used to study the effect of particle acidity on SOA formation from both biogenic and aromatic hydrocarbons.

Atmospheric aerosols always have a very complex composition. Studying the effects of $(NH_4)_2SO_4$ or H_2SO_4 seed aerosols did not draw the whole picture of the role that inorganic seed aerosols play in SOA formation. Metal-containing aerosols are important components of the atmosphere. Calcium and iron are the most abundant metal species in atmospheric aerosols and the average concentration of them in Beijing could be as high as about 1.2 μg m^{-3} and 1.1 μg/m^3 in $PM_{2.5}$ (He et al., 2001) respectively. In this study, we tested the effect of different inorganic seeds on SOA formation using a smog chamber. Two aromatic hydrocarbon precursors toluene and m-xylene are used. Effects of various inorganic seeds, including neutral inorganic seed $CaSO_4$, acidic seed $(NH_4)_2SO_4$, transition metal contained inorganic seeds $FeSO_4$ and $Fe_2(SO_4)_3$, and a mixture of $(NH_4)_2SO_4$ and $FeSO_4$, were examined during *m*-xylene or toluene photooxidation with the presence of nitrogen oxides (NO_x).

2. Experimental section

The experiments were carried out in a smog chamber which was described in detail in Wu et al. (Wu et al., 2007). The 2 m^3 cuboid reactor, with a surface-to-volume ratio of 5 m^{-1}, was constructed with 50 μm-thick FEP-Teflon film (Toray Industries, Inc. Japan). The reactor was located in a temperature controlled room (Escpec SEWT-Z-120), with a constant temperature between 10 and 60 °C (± 0.5 °C). The reactor was irradiated by 40 black lights (GE F40T12/BLB, peak intensity at 365 nm). Based on the equilibrium concentrations of NO, NO_2 and O_3 in a photo-irradiation experiment of an NO_2/air mixture, the NO_2 photolysis rate was calculated at approximately 0.21 min^{-1}, using a method described by Takekawa et al. (2000, 2003).

Prior to each experiment, the chamber was flushed for about 40 h with purified air at a flow rate of 15 L/min. In the first 20 hours, the chamber was exposed to UV light at 34 °C. In the last several hours of the flush, humid air was introduced to obtain the target relative humidity (RH).

Seed aerosols were generated by atomizing salt solutions using a constant output atomizer (TSI Model 3076). To avoid hydrolysis and precipitation in the $Fe_2(SO_4)_3$ salt solution, as little sulfuric acid as possible was added to the solution. What's more, for generating internally mixed seed aerosols, a mixed solution of $FeSO_4$ and $(NH_4)_2SO_4$, in which the concentration ratio of $FeSO_4$ to $(NH_4)_2SO_4$ is 1:5, was used. The generated aerosols were passed through a diffusion dryer (TSI Model 3062) to remove water and a neutralizer (TSI Model 3077) to bring the aerosols to an equilibrium charge distribution. The hydrocarbon, NO and NO_2 were carried by purified dry air into the chamber. The concentrations were continuously monitored at a measurement point in the reactor until they were stable, ensuring the components in the reactor were well mixed. The experiment was then conducted for 6 hours with the black lights on.

A gas chromatograph (GC, Beifen SP-3420) equipped with a DB-5 column (30 m×0.53 mm×1.5 mm, Dikma) and flame ionization detector (FID) measured the concentration of the hydrocarbon every 15 min. NO_x and O_3 were monitored with an interval of 1 min by a NO_x analyzer (Thermo Environmental Instruments, Model 42C) and an O_3 analyzer (Thermo Environmental Instruments, Model 49C), respectively. Size distribution of particle matter (PM) was measured by a scanning mobility particle sizer (SMPS, TSI 3936) in the range of 17-1000 nm with a 6-min cycle. The volume concentration of aerosols was estimated from the measured size distribution by assuming the particles were geometrically spherical and nonporous.

3. Results and discussion

3.1. Estimating the generated SOA mass (M_o)

Due to deposition of particles on the Teflon film, the measured aerosol concentration had to be corrected. Takekawa et al. (2003) developed a particle size-dependent correction method, in which the aerosol deposition rate constant ($k(d_p)$, h^{-1}) is a four-parameter function of particle diameter (d_p, nm), as shown in equation (1):

$$k(d_p) = a \bullet d_p^{\,b} + c \bullet d_p^{\,d} \quad (1)$$

The resulting $k(d_p)$ values for different d_p (40-700 nm) were determined by monitoring the particle number decay under dark conditions at low initial concentrations (<1000 particles cm^{-3}) to avoid serious coagulation. Based on more than 500 sets of $k(d_p)$ values (d_p ranges from 40 to 700 nm), the optimized values of parameter a, b, c, and d were calculated to be 6.46×10^{-7}, 1.78, 13.2, and -0.957, respectively. It should be noted that the estimation of deposited aerosol concentrations using this method might introduce some error (Takekawa et al., 2003) because some scatter was recognized when fitting $k(d_p)$ values into equation (1). To reduce error due to wall deposition, SOA yields were calculated when the measured particle concentration reached its maximum in the experiments because deposited aerosols were a greater proportion of the aerosol concentration change in the reactor after that time.

Several researchers have measured SOA density, providing an estimated range of 0.6-1.5 g cm^{-3} (Bahreini et al., 2005, Poulain et al., 2010, Qi et al., 2010, Song et al., 2007, Yu et al., 2008). In our study, we used a unit density (1.0 g cm^{-3}) to calculate SOA mass concentrations. This follows the approach used in Takekawa et al. (2003) and Verheggen et al. (2007).

3.2. Calculation of SOA yields

The fractional SOA yield (Y), defined as the ratio of the generated organic aerosol concentration (M_o) to the reacted hydrocarbon concentration (ΔHC), was used to represent the aerosol formation potential of the hydrocarbon (Pandis et al., 1992). Odum et al. (1996) developed a gas/particle absorptive partitioning model to describe the phenomenon that Y

largely depends on the amount of organic aerosol mass present. Equation (2) illustrates the relationship between SOA yield and organic aerosol mass concentration:

$$Y = \frac{\Delta M_o}{\Delta HC} = \frac{\sum_i A_i}{\Delta HC} = M_o \sum_i \frac{\alpha_i K_{om,i}}{1 + K_{om,i} M_o} \quad (2)$$

In equation (2), i presents the serial number of the hydrocarbon reaction products, A_i, α_i and $K_{om,i}$ (m^3 μg^{-1}) are the aerosol mass concentration, the stoichiometric coefficient based on mass and the normalized partitioning constant for product i respectively. If we assume that all semi-volatile products can be classified into one or two groups, equation (2) can be simplified to a one-product model (i.e., i=1) or two-product model (i.e., i=2). Parameters (α and K_{om}) can be obtained by fitting the experimental SOA yield data with a least square method. Since numerous compounds are actually produced by the reaction of a hydrocarbon, parameters obtained by the simplified model only represent the overall properties of all products (Odum et al., 1996). A one-product model was proved sufficiently accurate to describe the relationship between aerosol yield and mass (Henry et al., 2008, Takekawa et al., 2003, Verheggen et al., 2007). Therefore, we used a one-product model for our experimental SOA yield data to quantify of the effects of inorganic seed aerosols on SOA formation.

3.3. Effects of $CaSO_4$ and $(NH_4)_2SO_4$ seed aerosols on SOA formation

To investigate the effects of neutral and acid aerosols on SOA formation in *m*-xylene photooxidation, $CaSO_4$ and $(NH_4)_2SO_4$ were selected as surrogates. Experimental conditions were listed in Table 1. Six seed-free experiments (Xyl-N1~6), three $CaSO_4$-introduced experiments (Xyl-CS1~3) and nine $(NH_4)_2SO_4$-introduced experiments (Xyl-AS1~9) were carried out. Among these experiments, some experiments have identical initial conditions except for the seed aerosols (i.e. experiments Xyl-N5, Xyl-CS2, Xyl-AS2, Xyl-AS3, Xyl-AS9). Comparing the temporal variation of NO and O_3 during these experiments with similar initial conditions (Figure 1), the results indicate that $CaSO_4$ and $(NH_4)_2SO_4$ seed aerosols have no significant effect on gas-phase reactions. This result is consistent with the findings of Kroll et al. (2007) and Cao and Jang (2007) that $(NH_4)_2SO_4$ and $(NH_4)_2SO_4/H_2SO_4$ seed aerosols had a negligible effect on hydrocarbon oxidation.

Similarly, by comparing the temporal variation particle concentrations (Figure 2) during the experiments with identical initial conditions except for the seed aerosols, the effects of $CaSO_4$ and $(NH_4)_2SO_4$ seed aerosols on SOA formation were identified. In Figure 2, $PM_{corrected}$ was calculated from the measured PM concentrations plus wall deposit loss, and PM_0 was the seed aerosol concentration. The results indicate that the presence of neutral aerosols $CaSO_4$ (16-73μg m^{-3}) in the *m*-xylene/NO_x photooxidation system have no significant effect on SOA formation. Experiments with the presence of acid aerosols $(NH_4)_2SO_4$ have different particle profiles according to the concentrations of the introduced $(NH_4)_2SO_4$ seed aerosol. In Figure 2, experiment Xyl-AS2 has similar particle profile with the seed-free experiment Xyl-N5, indicating that $(NH_4)_2SO_4$ seed aerosols have little effect on SOA formation when the

initial concentration is low. However, when with high concentration of $(NH_4)_2SO_4$ seed aerosol introduced, SOA formation was enhanced (i.e. experiments Xyl-AS3 and Xyl-AS9) comparing with the seed-free experiment Xyl-N5. Comparing experiments Xyl-AS3 and Xyl-AS9, higher concentration of $(NH_4)_2SO_4$ seed aerosol resulted in higher SOA concentration. Therefore, the effects of $(NH_4)_2SO_4$ seed aerosol on SOA formation depend on its concentration.

Experiment no.	HC_0 (ppm)	PM_0 ($\mu m^3\ cm^{-3}$)	$PM_{0,S}$ ($cm^2\ m^{-3}$)	NO_0 (ppb)	$NO_{x,0}$ (ppb)	$HC_0/NO_{x,0}$	Mo ($\mu g\ m^{-3}$)	ΔHC (ppm)	Y (%)
Xyl-N1	0.92	0	-	72	148	6.2	66	0.27	5.6
Xyl-N2	1.26	0	-	102	209	6.0	92	0.32	6.7
Xyl-N3	1.74	0	-	137	276	6.3	122	0.39	7.3
Xyl-N4	1.68	0	-	132	272	6.2	125	0.39	7.5
Xyl-N5	2.00	0	-	161	333	6.0	148	0.45	7.6
Xyl-N6	2.51	0	-	182	381	6.6	191	0.54	8.3
Xyl-CS1	1.17	16	-	86	174	6.7	67	0.29	5.4
Xyl-CS2	2.03	43	-	167	343	5.9	148	0.46	7.6
Xyl-CS3	2.90	73	-	232	471	6.2	201	0.59	8.0
Xyl-AS1	2.85	11	3.5	208	420	6.8	208	0.57	8.6
Xyl-AS2	2.06	23	6.7	166	337	6.1	150	0.45	7.7
Xyl-AS3	2.15	47	11.0	162	326	6.6	169	0.45	8.8
Xyl-AS4	0.92	43	13.2	70	137	6.7	93	0.27	8.1
Xyl-AS5	1.73	45	12.8	132	272	6.4	165	0.40	9.7
Xyl-AS6	2.41	55	13.0	178	365	6.6	232	0.53	10.3
Xyl-AS7	0.92	63	16.7	70	143	6.4	110	0.26	10.1
Xyl-AS8	1.56	69	17.1	132	269	5.8	173	0.35	11.5
Xyl-AS9	2.07	74	17.1	166	348	6.0	249	0.47	12.3

Table 1. Initial experiment conditions and results for experiments with/without $CaSO_4$ or $(NH_4)_2SO_4$: initial m–xylene concentration (HC_0), initial seed aerosol mass concentration (PM_0), initial seed aerosol surface concentration ($PM_{0,S}$), initial NO_x concentrations (NO_0 and $NO_{x,0}$-NO_0), ratio of $HC_0/NO_{x,0}$, generated SOA mass (M_o), reacted hydrocarbon (ΔHC) , and SOA yield (Y)

Further analysis found that the effects of $(NH_4)_2SO_4$ seed aerosol on SOA yield were positively correlated with the surface concentration of $(NH_4)_2SO_4$ seed aerosols. To draw the SOA yield curves shown in Figure 3, the experiments were classified into different groups (experiment Xyl-AS3 was not classified into any group since the surface concentration of $(NH_4)_2SO_4$ seed aerosols in this experiment was different from others) by the surface concentration of $(NH_4)_2SO_4$ seed aerosols. The regression lines for each group (there was no regression line for experiments XylCS1~2 and Xyl-AS1~3 since they had similar SOA yield with the seed-free experiments) were produced by fitting the data of generated SOA mass (M_o) and SOA yield (Y) into a one-product partition model. As indicated in Figure 3, experiments with higher surface concentration of $(NH_4)_2SO_4$ seed aerosols had higher yield curves. As proposed by most research, acid-catalyzed aerosol-phase reactions (Cao and

Jang, 2007, Czoschke et al., 2003, Gao et al., 2004) and uptake of semivolatile organic products to acidic sulfate aerosols enhance SOA formation (Liggio and Li, 2008). The observed SOA formation enhancement could be related to the acid catalytic effect of $(NH_4)_2SO_4$ seeds on particle-phase surface heterogeneous reactions and the surface uptake of semivolatile organic products.

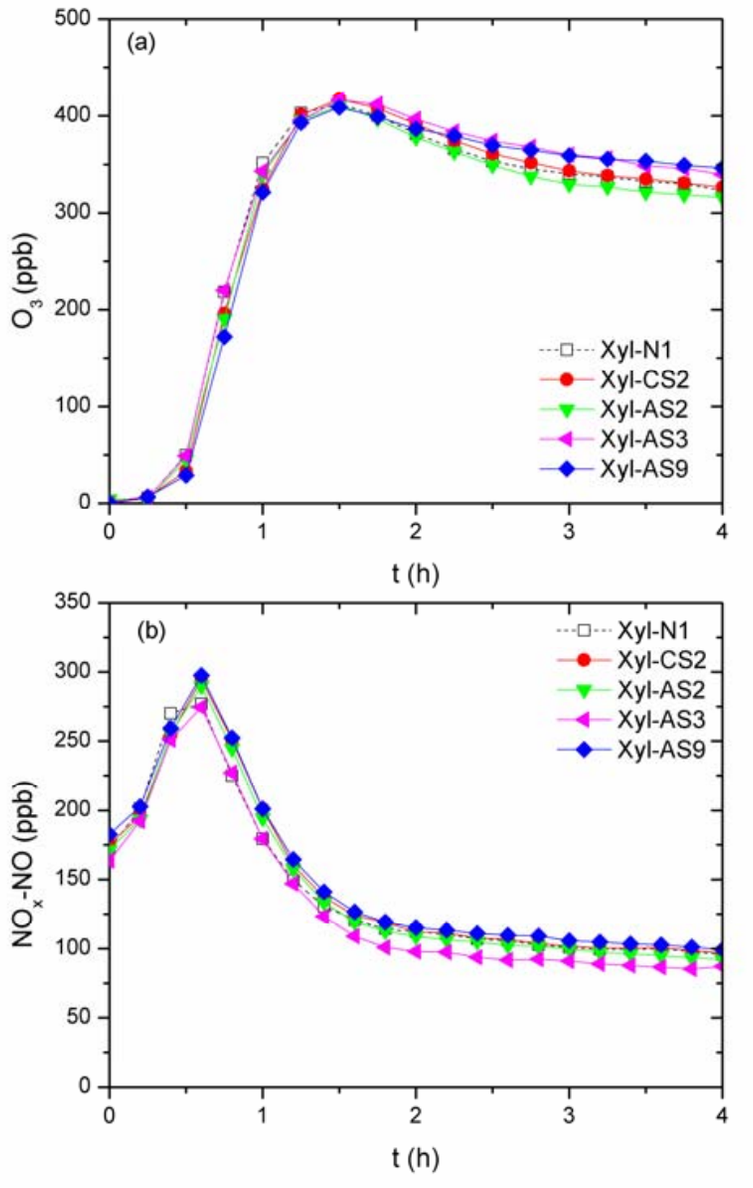

Figure 1. Temporal evolutions of O_3 (a) and NO_x-NO (b) concentration in experiments with/without $CaSO_4$ and $(NH_4)_2SO_4$ seed aerosols

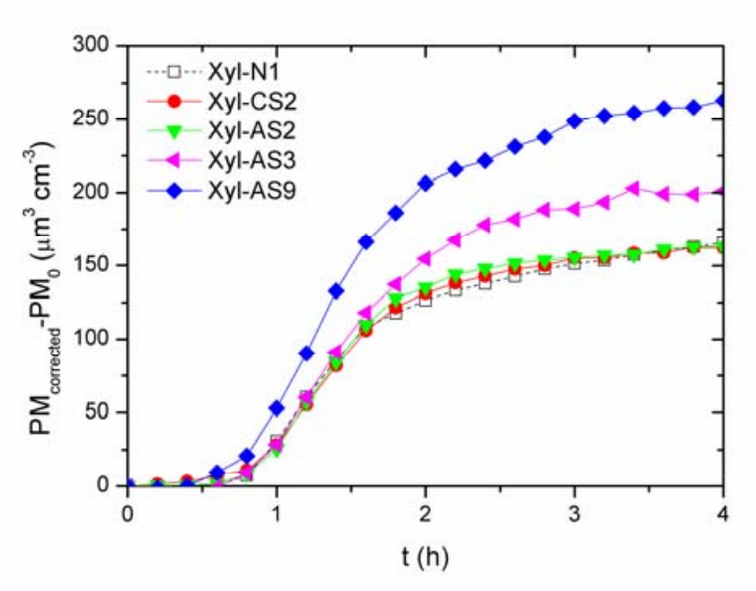

Figure 2. Temporal evolutions of generated particle concentration in experiments with/without $CaSO_4$ and $(NH_4)_2SO_4$ seed aerosols

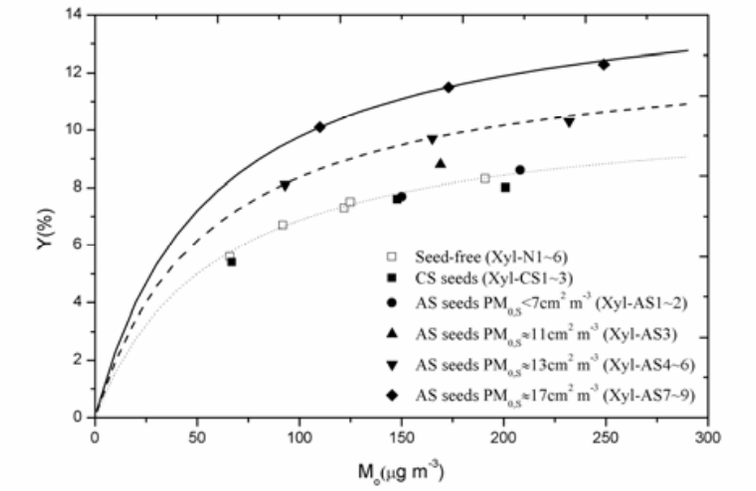

Figure 3. SOA yields (Y) from photooxidation of m-xylene versus organic aerosol mass (Mo) for experiments with/without $CaSO_4$ and $(NH_4)_2SO_4$ seed aerosols

3.4. Effects of $Fe_2(SO_4)_3$ and $FeSO_4$ seed aerosols on SOA formation

A seed-free experiment and three experiments with $Fe_2(SO_4)_3$ seed aerosols were carried out to investigate $Fe_2(SO_4)_3$ seed aerosols on phooxidation of toluene/NO_x. The four experiments had identical initial conditions except for the concentrations of the introduced $Fe_2(SO_4)_3$ seed aerosol. $Fe_2(SO_4)_3$ seed aerosols did not have obvious effects on SOA formation as shown in the temporal variation of $PM_{corrected}$–PM_0 concentrations in Figure 4. $Fe_2(SO_4)_3$ seed aerosols had no obvious effect on gas phase compounds in toluene/NO_x photooxidation either. A minimal amount of acid was added to the solution to generate $Fe_2(SO_4)_3$ seed aerosols. The introduced H^+ concentration was in the range of 0.0002-0.002 μg m^{-3} in the $Fe_2(SO_4)_3$-

introduced experiments. This is much lower than the H^+ concentration in the "non-acid" experiment by Cao and Jang (2007). Therefore, we presume the effect of the introduced sulfuric acid was negligible and $Fe_2(SO_4)_3$ seed aerosols did not have obvious effects on SOA formation in phooxidation of toluene/NO_x.

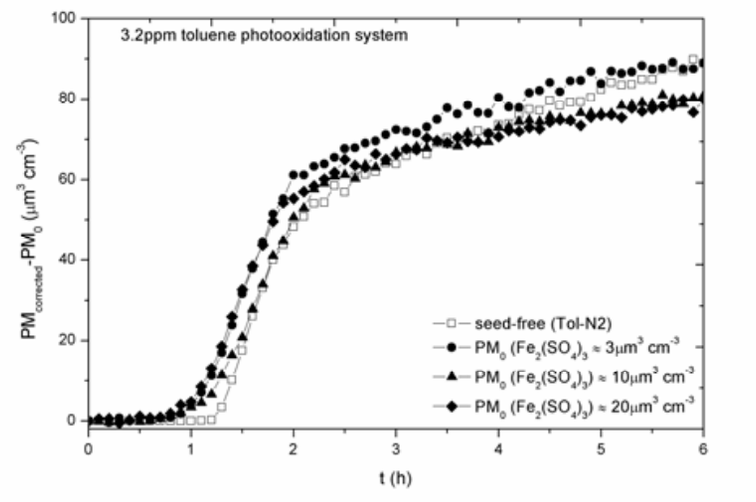

Figure 4. Variations of generated SOA mass as a function of time from toluene/NO_x photooxidation with different concentrations of $Fe_2(SO_4)_3$ seed aerosols

We also conducted 18 irradiated toluene/NO_x experiments with/without $FeSO_4$ seed aerosols. The conditions, generated SOA mass (M_o), and SOA yield (Y) are shown in Table 2. $FeSO_4$ seed aerosols had no obvious effect on gas phase compounds either, but significantly suppressed SOA formation. Figure 5 compares the temporal variation of particle concentrations during the 4.2 ppm toluene experiments (Exierments Tol-N3, Tol-FS1, Tol-FS3, Tol-FS8 and Tol-FS12) conducted under identical initial conditions except seed aerosol concentrations. Experiments with the presence of $FeSO_4$ seed aerosol generated less SOA than the seed-free experiment. And experiment with a higher $FeSO_4$ seed aerosol concentration generated less SOA than experiment with a lower $FeSO_4$ concentration. So the inhibited effect of $FeSO_4$ aerosols on SOA yield became stronger at higher concentrations of $FeSO_4$ seed aerosols. At other toluene/NO_x photooxidation concentrations, we also found similar temporal variation of particle concentrations. However, as indicated in Table 2 and Figure 5, SOA yields of experiments Tol-FS1 and Tol-FS3 are similar to corresponding seed-free experiments of Tol-N3. These two seed-introduced experiments (as well as Tol-FS2) were conducted at the lowest ratio of $FeSO_4$ seed aerosol mass concentration to initial toluene mass concentration ($FeSO_4$/toluene) and did not show obvious effect on SOA formation comparing to their corresponding seed-free experiments. In these three experiments, the mass ratios of $FeSO_4$/toluene (assuming particle density to be 1.898 g cm^{-3}, density of $FeSO_4 \cdot 7H_2O$, because of the lack of the information the amount of hydrate water) were calculated to be lower than 4.2×10^{-4}. It is possible that most of the ferrous iron was oxidized before significant SOA mass were generated since few $FeSO_4$ seed aerosols were introduced and high concentrations of oxidizing substances were generated during the

toluene/NO_x photooxidation. Besides these three experiments with lowest $FeSO_4$/toluene mass ratio, $FeSO_4$ seed aerosols suppressed SOA formation relative to the corresponding seed-free experiments. And in our experiments, the suppress ratio could be as high as 60%, as calculated from Table 2.

Experiment No.	HC_0 ppm	PM_0 $\mu m^3\ cm^{-3}$	NO_0 ppb	$NO_{x,0}$-NO_0 ppb	PM_0/ HC_0	$HC_0/NO_{x,0}$ ppm ppm^{-1}	M_o $\mu g\ m^{-3}$	ΔHC ppm	Y %
Tol-N1	1.10	0	50	51	0	11.0	26	0.20	3.8
Tol-FS4	1.08	1	51	50	5.1×10^{-4}	10.7	17	0.22	2.3
Tol-FS10	1.07	4	55	47	1.7×10^{-3}	10.6	14	0.20	2.2
Tol-FS14	1.09	10	48	49	4.4×10^{-3}	11.1	8	0.19	1.7
Tol-N2	3.30	0	165	160	0	10.2	90	0.48	5.0
Tol-FS5	3.21	4	160	162	6.1×10^{-4}	10.0	74	0.51	3.9
Tol-FS7	3.31	6	154	162	8.4×10^{-4}	10.5	72	0.56	3.5
Tol-FS9	3.19	11	164	157	1.5×10^{-3}	9.9	59	0.47	3.3
Tol-FS11	3.28	21	158	165	3.0×10^{-3}	10.2	36	0.51	1.9
Tol-N3	4.12	0	217	210	0	9.7	123	0.57	5.8
Tol-FS1	4.23	1	208	207	1.4×10^{-4}	10.2	105	0.57	5.0
Tol-FS3	4.25	4	208	213	4.2×10^{-4}	10.1	115	0.60	5.2
Tol-FS8	4.25	10	216	209	1.1×10^{-3}	10.0	81	0.55	4.0
Tol-FS12	4.23	27	213	210	3.0×10^{-3}	10.0	47	0.61	2.1
Tol-N4	6.10	0	287	293	0	10.5	189	0.96	6.3
Tol-FS2	6.05	5	295	306	3.5×10^{-4}	10.1	170	0.81	6.5
Tol-FS6	6.09	10	299	306	7.6×10^{-4}	10.1	140	0.88	4.8
Tol-FS13	6.03	41	296	310	3.2×10^{-3}	10.0	64	0.82	2.7

Table 2. Experimental conditions and results in toluene photooxidation: initial toluene concentration (HC_0), initial $FeSO_4$ seed aerosol concentration (PM_0), initial NO_x concentrations (NO_0 and $NO_{x,0}$-NO_0), ratio of PM_0/ HC_0, ratio of $HC_0/NO_{x,0}$, generated SOA mass (M_o), reacted hydrocarbon (ΔHC) , and SOA yield (Y)

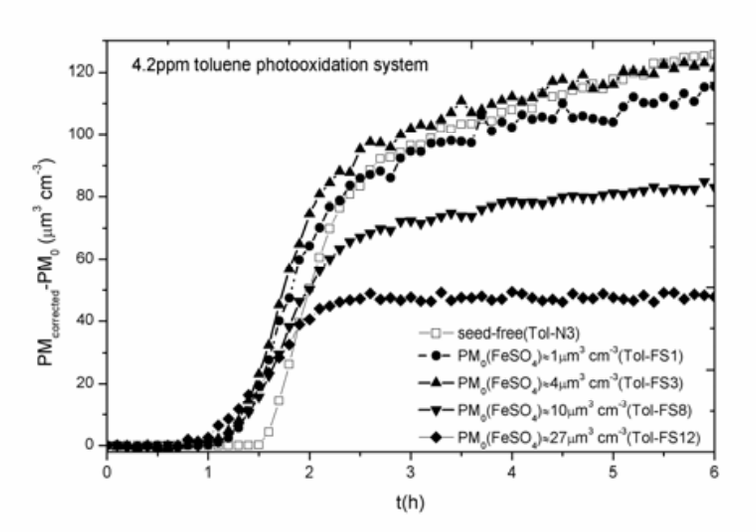

Figure 5. Temporal evolutions of SOA generation from toluene/NO_x photooxidation with different concentrations of $FeSO_4$ seed aerosols

We classified the experiments with $FeSO_4$ seed aerosols introduced into three groups by $FeSO_4$/toluene mass ratios to create SOA yield variations as a function of generated SOA mass (Figure 6). Experiments with different $FeSO_4$/toluene mass ratios seemed to fall into different yield curves. When $FeSO_4$/toluene mass ratio was lower than 4.2×10^{-4}, $FeSO_4$ seed aerosols had a negligible effect and SOA yields of these experiments with $FeSO_4$ seed aerosols coincide with the yield curve of seed-free experiments. When $FeSO_4$/toluene mass ratio was higher than 5.1×10^{-4}, the SOA yield curve indicated experiments with $FeSO_4$ seed aerosols had lower yields than seed-free experiments. Lower yield curves from the experiments with higher $FeSO_4$/toluene mass ratio were observed, indicating that a higher Fe/C ratio had a greater suppression effect on SOA formation from toluene/NO_x photooxidation.

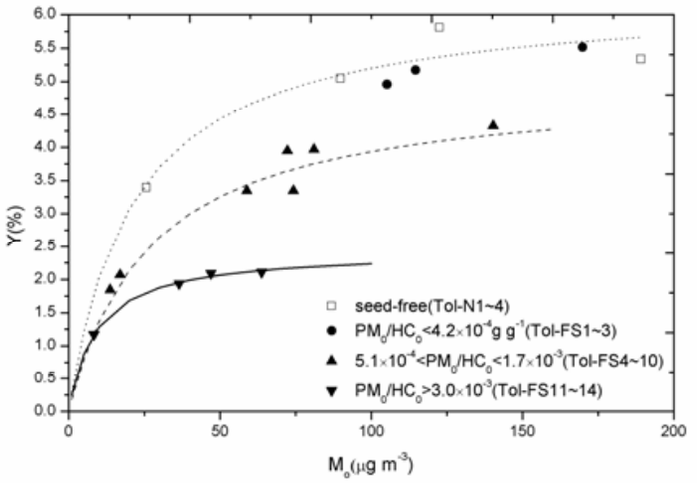

Figure 6. SOA yield (Y) variations as a function of generated SOA mass (M_o) from toluene/NO_x photooxidation with/without $FeSO_4$ seeds

3.5. Effects of mixed $(NH_4)_2SO_4$ and $FeSO_4$ aerosols on SOA formation

Atmospheric aerosol is often a mixture of different components. We tested the effect of internal mixed $(NH_4)_2SO_4$ and $FeSO_4$ seed aerosols on SOA formation in *m*-xylene/NO_x photooxidaiton. The experimental conditions, generated SOA mass (M_o), and SOA yield (Y) are shown in Table 3. To generate internal mixed $(NH_4)_2SO_4$ and $FeSO_4$ aerosols, a mixed solution of $(NH_4)_2SO_4$ and $FeSO_4$, in which the mass concentration ratio of $(NH_4)_2SO_4$ to $FeSO_4$ was 5:1, was used in the atomizer. So the approximately 60 μm^3 cm^{-3} seed aerosols in the three experiments with mixed $(NH_4)_2SO_4$ and $FeSO_4$ seed aerosols (Xyl-FA1~3) contained about 10 μm^3 cm^{-3} $FeSO_4$ seed aerosols and 50 μm^3 cm^{-3} $(NH_4)_2SO_4$ seed aerosols.

As mentioned above, neither $(NH_4)_2SO_4$ seed aerosols nor $FeSO_4$ seed aerosols had obvious effects on gas phase compounds. And in the experiments in this section, we found that mixed $(NH_4)_2SO_4$ and $FeSO_4$ seed aerosols had no obvious effect on gas phase compounds either.

In Figure 7, after wall deposition correction and deduction of seed aerosols, temporal variation of particle concentrations in experiments conducted under identical initial conditions except seed aerosol concentrations (the initial concentration of *m*-xylene is 1.1ppm, 2.1ppm and 3.2 ppm in picture a, b and c, respectively) were compared.

Experiment No.	HC_0 ppm	PM_0 $\mu m^3\ cm^{-3}$	NO_0 ppb	$NO_{x,0}$-NO_0 ppb	$HC_0/NO_{x,0}$ ppm ppm^{-1}	M_o $\mu g\ m^{-3}$	ΔHC ppm	Y %
Xyl-N7	1.08	0	62	62	8.7	21	0.30	1.7
Xyl-FS1	1.01	7	58	63	8.4	8	0.29	0.7
Xyl-AS10	1.07	44	63	65	8.3	51	0.32	3.7
Xyl-FA1	1.05	62	64	69	7.9	30	0.31	2.3
Xyl-N8	2.07	0	121	120	8.6	57	0.39	3.4
Xyl-FS2	2.09	9	119	121	8.7	29	0.42	1.6
Xyl-AS11	2.15	53	121	119	9.2	119	0.52	5.4
Xyl-FA2	2.09	66	123	125	8.5	56	0.43	3.1
Xyl-N9	3.21	0	198	180	8.5	145	0.74	4.6
Xyl-FS3	3.23	11	188	182	8.8	48	0.63	1.8
Xyl-AS12	3.10	48	182	178	8.5	213	0.71	7.0
Xyl-FA3	3.16	57	179	186	8.7	117	0.74	3.7

Table 3. Experimental conditions and results in toluene photooxidation: initial toluene concentration (HC_0), initial $FeSO_4$ seed aerosol concentration (PM_0), initial NO_x concentrations (NO_0 and $NO_{x,0}$-NO_0), ratio of $HC_0/NO_{x,0}$, generated SOA mass (M_o), reacted hydrocarbon (ΔHC) and SOA yield (Y)

As indicated in Figure 7(a), comparing with the seed-free experiment Xyl-N7, both experiment Xyl-AS10 and experiment Xyl-FA1 had higher particle concentrations while experiment Xyl-FS1 had lower particle concentrations. So, in 1.1ppm *m*-xylene photooxidation, the presence of $(NH_4)_2SO_4$ aerosols and mixed aerosols (mixed $(NH_4)_2SO_4$ and $FeSO_4$) both increased SOA formation, while the presence of $FeSO_4$ suppressed SOA formation. In Figure 7(b) and Figure 7(c), the effects of single $(NH_4)_2SO_4$ seed aerosols (promotion effect) and single $FeSO_4$ seed aerosols (suppression effect) on SOA formation were consistent with Figure 7(a). However, the mixed aerosols seemed to have different effects on SOA formation in photooxidation systems with different initial concentrations of *m*-xylene. In Figure 7(b), experiment Xyl-FA2 had similar temporal variation of particle concentrations with its corresponding seed-free experiment Xyl-N8, and in Figure 7(c), experiment Xyl-FA3 had lower temporal variation of particle concentrations than its corresponding seed-free experiment Xyl-N9. It must be noted that the seed aerosols in experiments Xyl-FA1~3 had similar concentrations and components. So, aerosols at the same mixing ratio of $(NH_4)_2SO_4$ and $FeSO_4$ could either enhance or suppress SOA formation depending on the experimental conditions. It seemed that the promotion effect of $(NH_4)_2SO_4$ aerosols and the suppression effect of $FeSO_4$ aerosols competed when both of them existed. And the promotion effect of $(NH_4)_2SO_4$ aerosols was dominant with low initial hydrocarbon concentration in the competition, while the reverse was true with high initial hydrocarbon concentration. This illustrates that the interplay of different compositions of real atmosphere aerosols can lead to complex synergistic effects on SOA formation.

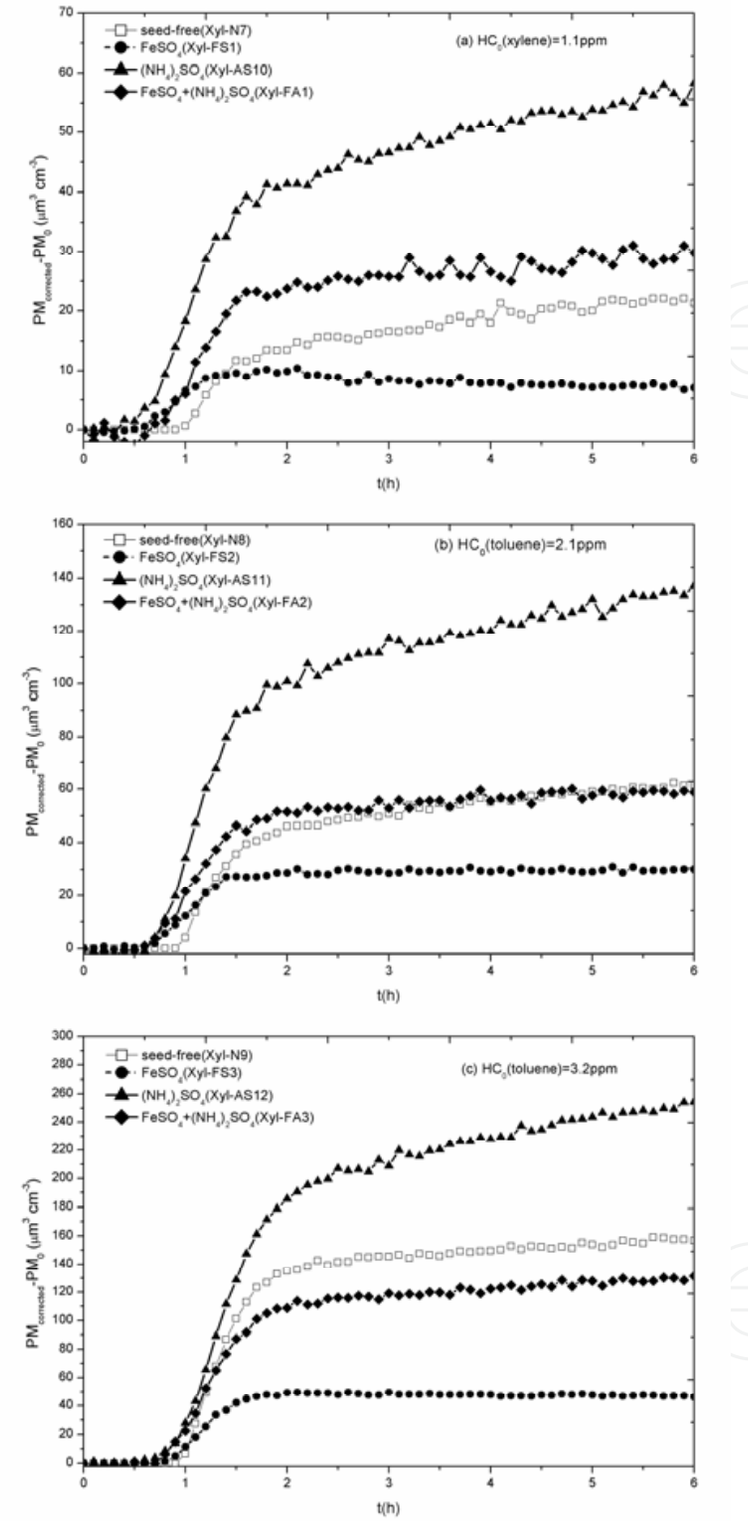

Figure 7. Temporal evolutions of generated particle concentration in experiments with/without $FeSO_4$, $(NH_4)_2SO_4$ and mixed $FeSO_4$ and $(NH_4)_2SO_4$ seed aerosols

According to the composition of the seed aerosols, experiments with inorganic seed aerosols introduced were classified into three groups. In Figure 8, SOA yield (Y) variations as a function of generated SOA mass (M_o) from *m*-xylene/NO_x photooxidation were plotted. The

regression lines for each group were produced by fitting the data of generated SOA mass (M_o) and SOA yield (Y) into a one-product partition model. As indicated in Figure 8, experiments with the presence of $(NH_4)_2SO_4$ had a higher SOA yield curve than the seed-free experiments, while experiments with the presence of $FeSO_4$ seed aerosols had a lower one, indicating the presence of $(NH_4)_2SO_4$ and $FeSO_4$ seed aerosols increased and decreased SOA yield, respectively. For the experiments with mixed seed aerosols, their SOA yield curve was similar to or a little higher than the seed-free experiments when the SOA mass load was low, but their SOA yield curve was lower than the seed-free experiments when the SOA mass load was high.

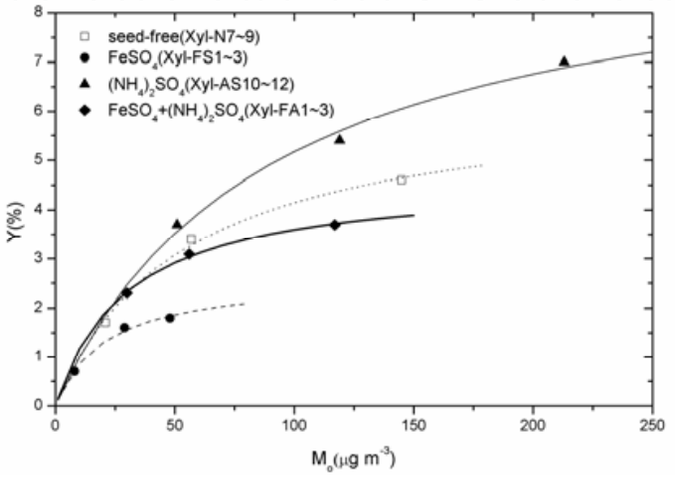

Figure 8. SOA yield (Y) variations as a function of generated SOA mass (M_o) from *m*-xylene/NO_x photooxidation with/without $FeSO_4$, $(NH_4)_2SO_4$ and mixed $FeSO_4$ and $(NH_4)_2SO_4$ seed aerosols

3.6. Hypothesis for inorganic seed aerosols' effects

In our experiment, we observed that $FeSO_4$ seed aerosols suppressed SOA formation while $Fe_2(SO_4)_3$ seed aerosols had no effect on SOA formation. It appears that the inhibiting effect of Fe(II) involves its strong reducing properties. Hydrocarbon precursors are oxidized by OH·, NO_3·, etc. During the gas phase reaction, the oxidized products usually have a lower saturation vapor pressure and, as a result, condense to the aerosol phase. When these oxidized condensable compounds (CCs) containing carbonyl, hydroxyl, and carboxyl groups (Gao et al., 2004, Hamilton et al., 2005) contact ferrous iron in the aerosol phase, they may react to produce ferric iron and less condensable compounds (LCCs) or incondensable compounds (ICs). The ferrous iron may stop some CCs from being further oxidized and forming low-volatility products (Hallquist et al., 2009), including oligomers (Gao et al., 2004). The experimental results also showed that the presence of neutral $CaSO_4$ seed aerosols seed aerosols have no significant effect on photooxidation of aromatic hydrocarbons, while the presence of acid $(NH_4)_2SO_4$ seed aerosols can significantly enhance SOA generation and SOA yield. A possible mechanism is shown in Figure 9. Oligomerization is one important step during SOA formation (Nguyen et al., 2011). As proposed by (Kroll et al., 2007), the effect of $(NH_4)_2SO_4$ seed aerosols may be attributed to acid catalyzed particle-phase reactions, forming high molecular weight, low-volatility products (e.g. oligomers). These processes may deplete the semivolatile CCs in the particle phase, and enhance SOA formation by shifting the gas-particle equilibrium, which is shown in

Figure 9, and, therefore force more CCs condense to aerosol phase. Since $(NH_4)_2SO_4$ and $FeSO_4$ seed aerosols may both influence the semivolatile CCs, there is a competition for CCs to form higher-volatility products (LCCs or ICs) or low-volatility products (e.g. oligomers).

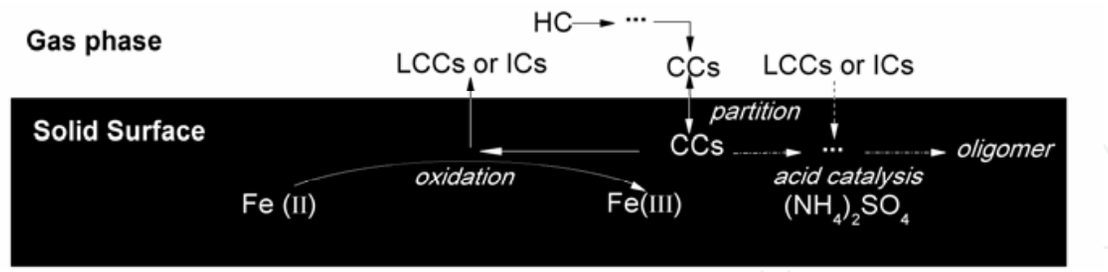

Figure 9. Hypothesized mechanism for inorganic seed aerosols' effects on SOA formation: ferrous iron Fe (II) reduces or decompose some condensable compounds (CCs), which are oligomer precursors, interrupting oligomerization and generating high volatility products (LCCs or ICs); while acid seed aerosols catalyze aerosol-phase reactions, generating oligomeric products

4. Conclusion

Effects of various inorganic seeds, including neutral inorganic seed $CaSO_4$, acidic seed $(NH_4)_2SO_4$, transition metal contained inorganic seeds $FeSO_4$ and $Fe_2(SO_4)_3$, and a mixture of $(NH_4)_2SO_4$ and $FeSO_4$, were examined during *m*-xylene or toluene photooxidation. Our results indicate that the presence of $CaSO_4$ seed aerosols and $Fe_2(SO_4)_3$ seed aerosols have no effect on photooxidation of aromatic hydrocarbons, while the presence of $(NH_4)_2SO_4$ seed aerosols and $FeSO_4$ seed aerosols have no effect on gas-phase reactions, but can significantly influence SOA generation and SOA yields. $(NH_4)_2SO_4$ seed aerosols enhance SOA formation and increase SOA yield due to acid catalytic effect of $(NH_4)_2SO_4$ seeds on particle-phase surface heterogeneous reactions. While $FeSO_4$ seed aerosols suppress SOA formation and decrease SOA yield possibly due to the reduction of some oligomer precursor CCs. These results reveal that many inorganic seeds are not inert during photooxidation process and can significantly influence SOA formation. These observed effects can be incorporated into air quality models to improve their accuracy in predicting SOA and fine particle concentrations.

Author details

Biwu Chu, Jingkun Jiang*, Zifeng Lu, Kun Wang, Junhua Li and Jiming Hao
State Key Laboratory of Environment Simulation and Pollution Control, School of Environment, Tsinghua University, Beijing, China

Acknowledgement

This work was supported by the National Natural Science Fundation of China (20937004, 21107060, and 21190054), Toyota Motor Corporation and Toyota Central Research and Development Laboratories Inc.

* Corresponding Author

5. References

Bahreini, R., Keywood, M.D., Ng, N.L., Varutbangkul, V., Gao, S., Flagan, R.C., Seinfeld, J.H., Worsnop, D.R., Jimenez, J.L., 2005. Measurements of secondary organic aerosol from oxidation of cycloalkenes, terpenes, and m-xylene using an Aerodyne aerosol mass spectrometer. Environmental Science & Technology 39, 5674-5688.

Cao, G., Jang, M., 2007. Effects of particle acidity and UV light on secondary organic aerosol formation from oxidation of aromatics in the absence of NOx. Atmospheric Environment 41, 7603-7613.

Cheng, S.-h., Yang, L.-x., Zhou, X.-h., Xue, L.-k., Gao, X.-m., Zhou, Y., Wang, W.-x., 2011. Size-fractionated water-soluble ions, situ pH and water content in aerosol on hazy days and the influences on visibility impairment in Jinan, China. Atmospheric Environment 45, 4631-4640.

Czoschke, N.M., Jang, M., Kamens, R.M., 2003. Effect of acidic seed on biogenic secondary organic aerosol growth. Atmospheric Environment 37, 4287-4299.

Duan, F.K., He, K.B., Ma, Y.L., Jia, Y.T., Yang, F.M., Lei, Y., Tanaka, S., Okuta, T., 2005. Characteristics of carbonaceous aerosols in Beijing, China. Chemosphere 60, 355-364.

Gao, S., Ng, N.L., Keywood, M., Varutbangkul, V., Bahreini, R., Nenes, A., He, J.W., Yoo, K.Y., Beauchamp, J.L., Hodyss, R.P., Flagan, R.C., Seinfeld, J.H., 2004. Particle phase acidity and oligomer formation in secondary organic aerosol. Environmental Science & Technology 38, 6582-6589.

Hallquist, M., Wenger, J.C., Baltensperger, U., Rudich, Y., Simpson, D., Claeys, M., Dommen, J., Donahue, N.M., George, C., Goldstein, A.H., Hamilton, J.F., Herrmann, H., Hoffmann, T., Iinuma, Y., Jang, M., Jenkin, M.E., Jimenez, J.L., Kiendler-Scharr, A., Maenhaut, W., McFiggans, G., Mentel, T.F., Monod, A., Prevot, A.S.H., Seinfeld, J.H., Surratt, J.D., Szmigielski, R., Wildt, J., 2009. The formation, properties and impact of secondary organic aerosol: current and emerging issues. Atmospheric Chemistry and Physics 9, 5155-5236.

Hamilton, J.F., Webb, P.J., Lewis, A.C., Reviejo, M.M., 2005. Quantifying small molecules in secondary organic aerosol formed during the photo-oxidation of toluene with hydroxyl radicals. Atmospheric Environment 39, 7263-7275.

He, K.B., Yang, F.M., Ma, Y.L., Zhang, Q., Yao, X.H., Chan, C.K., Cadle, S., Chan, T., Mulawa, P., 2001. The characteristics of PM2.5 in Beijing, China. Atmospheric Environment 35, 4959-4970.

Henry, F., Coeur-Tourneur, C., Ledoux, F., Tomas, A., Menu, D., 2008. Secondary organic aerosol formation from the gas phase reaction of hydroxyl radicals with m-, o- and p-cresol. Atmospheric Environment 42, 3035-3045.

Jang, M.S., Czoschke, N.M., Lee, S., Kamens, R.M., 2002. Heterogeneous atmospheric aerosol production by acid-catalyzed particle-phase reactions. Science 298, 814-817.

Kaiser, J., 2005. How dirty air hurts the heart. Science 307, 1858-1859.

Kroll, J.H., Chan, A.W.H., Ng, N.L., Flagan, R.C., Seinfeld, J.H., 2007. Reactions of semivolatile organics and their effects on secondary organic aerosol formation. Environmental Science & Technology 41, 3545-3550.

Lewandowski, M., Jaoui, M., Offenberg, J.H., Kleindienst, T.E., Edney, E.O., Sheesley, R.J., Schauer, J.J., 2008. Primary and secondary contributions to ambient PM in the midwestern United States. Environmental Science & Technology 42, 3303-3309.

Liggio, J., Li, S.M., 2008. Reversible and irreversible processing of biogenic olefins on acidic aerosols. Atmospheric Chemistry and Physics 8, 2039-2055.

Nguyen, T.B., Roach, P.J., Laskin, J., Laskin, A., Nizkorodov, S.A., 2011. Effect of humidity on the composition of isoprene photooxidation secondary organic aerosol. Atmospheric Chemistry and Physics 11, 6931-6944.

Odum, J.R., Hoffmann, T., Bowman, F., Collins, D., Flagan, R.C., Seinfeld, J.H., 1996. Gas/particle partitioning and secondary organic aerosol yields. Environmental Science & Technology 30, 2580-2585.

Pandis, S.N., Harley, R.A., Cass, G.R., Seinfeld, J.H., 1992. Secondary organic aerosol formation and transport. Atmospheric Environment Part a-General Topics 26, 2269-2282.

Poulain, L., Wu, Z., Petters, M.D., Wex, H., Hallbauer, E., Wehner, B., Massling, A., Kreidenweis, S.M., Stratmann, F., 2010. Towards closing the gap between hygroscopic growth and CCN activation for secondary organic aerosols - Part 3: Influence of the chemical composition on the hygroscopic properties and volatile fractions of aerosols. Atmospheric Chemistry and Physics 10, 3775-3785.

Qi, L., Nakao, S., Malloy, Q., Warren, B., Cocker, D.R., III, 2010. Can secondary organic aerosol formed in an atmospheric simulation chamber continuously age? Atmospheric Environment 44,

Satheesh, S.K., Moorthy, K.K., 2005. Radiative effects of natural aerosols: A review. Atmospheric Environment 39, 2089-2110.

Song, C., Na, K., Warren, B., Malloy, Q., Cocker, D.R., 2007. Secondary organic aerosol formation from m-xylene in the absence of NOx. Environmental Science & Technology 41, 7409-7416.

Takekawa, H., Karasawa, M., Inoue, M., Ogawa, T., Esaki, Y., 2000. Product analysis of the aerosol produced by photochemical reaction of α-pinene. Earozoru Kenkyu 15, 35-42.

Takekawa, H., Minoura, H., Yamazaki, S., 2003. Temperature dependence of secondary organic aerosol formation by photo-oxidation of hydrocarbons. Atmospheric Environment 37, 3413-3424.

Verheggen, B., Mozurkewich, M., Caffrey, P., Frick, G., Hoppel, W., Sullivan, W., 2007. alpha-Pinene oxidation in the presence of seed aerosol: Estimates of nucleation rates, growth rates, and yield. Environmental Science & Technology 41, 6046-6051.

Volkamer, R., Jimenez, J.L., San Martini, F., Dzepina, K., Zhang, Q., Salcedo, D., Molina, L.T., Worsnop, D.R., Molina, M.J., 2006. Secondary organic aerosol formation from anthropogenic air pollution: Rapid and higher than expected. Geophysical Research Letters 33, L17811.

Wu, S., Lu, Z.F., Hao, J.M., Zhao, Z., Li, J.H., Hideto, T., Hiroaki, M., Akio, Y., 2007. Construction and characterization of an atmospheric simulation smog chamber. Advances in Atmospheric Sciences 24, 250-258.

Yu, Y., Ezell, M.J., Zelenyuk, A., Imre, D., Alexander, L., Ortega, J., D'Anna, B., Harmon, C.W., Johnson, S.N., Finlayson-Pitts, B.J., 2008. Photooxidation of alpha-pinene at high relative humidity in the presence of increasing concentrations of NOx. Atmospheric Environment 42, 5044-5060.